

Composition and Morphology Changes and their Influence on Hydrogen Evolution on Ni-Mo and Fe-Mo Alloys Electrodeposited by DC and Pulsed Current

V. D. Jovic, B. M. Jovic, G. R. Stafford, Materials Science and Engineering Laboratory, National Institute of Standards and Technology, Gaithersburg, MD 20899, USA, N. V. Krstajic, Faculty of Technology and Metallurgy University of Belgrade, 11000 Belgrade, Karnegijeva 4, Yugoslavia and Z. Twardowski, Research & Development, Kvaerner Chemetics, 1818 Cornwall Avenue, Vancouver, BC, Canada V6J 1C7*

Ni-Mo and Fe-Mo alloys were electrodeposited using both DC and pulsed current from a pyrophosphate bath. Their composition and morphology were investigated by EDS and optical microscopy, respectively, in order to determine the influence of the deposition conditions on the morphology and composition of these alloys. It was shown that the electrodeposition parameters influenced both the composition of Fe-Mo alloys and the current efficiency for their deposition, while the macro-morphology did not change significantly with different applied current densities and waveforms. In the case of Ni-Mo alloys produced by pulse plating, the composition, morphology and current efficiency were all dependent on the applied current density. Compositions ranging from 28 at. % to 41 at. % Mo were obtained at current efficiencies less than 10%. When the Mo^{6+} concentration in the electrolyte was increased, the dependence of composition on current density was significantly reduced for both DC and pulsed plating. Even with the increased Mo^{6+} concentration, the current efficiency for DC plating remained below 10%. The morphology was particularly sensitive to the co-generation of hydrogen and most deposits were micro-cracked.

It was found that electrodeposited Fe-Mo alloys possess about 0.15 V lower overvoltage than mild steel for hydrogen evolution in an electrolyte commonly used in commercial chlorate production. The hydrogen evolution overvoltage for electrodeposited Ni-Mo alloys in sodium hydroxide solution was dependent on both the electrode composition and roughness, both of which were dependent on the deposition parameters. Preliminary electrochemical impedance spectroscopy (EIS) results recorded during hydrogen evolution on freshly deposited samples indicate that cracks present in the Ni-Mo coatings do not create diffusion barriers and limit the hydrogen evolution reaction. The impedance data was fit to an equivalent circuit that has successfully been used for EIS analysis of cast Ni-Mo alloys.

*** For more information, contact:**

V. D. Jovic
Materials Science and Engineering Laboratory
NIST
100 Bureau Drive
Gaithersburg, MD 20899
e-mail: vladimir.jovic@nist.gov
Tel: (301)-975-4874
Fax: (301)-926-7679

1. Introduction

Binary and ternary alloys containing transition metals such as Mo, W, Ni, Co, Fe, electrodeposited under direct current (DC) conditions, have been described in the literature as promising cathodes for hydrogen evolution in chlor-alkaline and chlorate electrolysis¹⁻⁴. It has been shown that certain deposit compositions tend to lower the hydrogen evolution overvoltage and it is anticipated that these new cathodic materials may perform better than those used commercially in industrial plants⁴.

The influence of pulse plating on current efficiency, composition and deposit morphology has also been examined⁵. A square wave pulsing regime has been used to produce Co-Mo alloy coatings containing up to 55 at. % molybdenum. Due to the co-generation of hydrogen at these deposition potentials, deposit current efficiencies of about 50% are typical. Deposits of poor quality were obtained using deposition current densities higher than 15 Adm^{-2} while micro-cracked, compact coatings were obtained at current densities of 2.5 Adm^{-2} to 15 Adm^{-2} . The polarization characteristics of coatings deposited at high frequency (10^4 Hz) using an effective current density of 2.5 Adm^{-2} have been investigated in electrolytes commonly used in brine electrolysis. It was shown that the overvoltage for hydrogen evolution on the Co-Mo alloy is about 0.15 V lower than that observed on mild steel⁶.

In this paper the morphology, composition, and hydrogen evolution kinetics for Fe-Mo and Ni-Mo alloy thin films were examined for a variety of electrodeposition conditions.

2. Experimental

All samples were deposited on mild steel substrates having a surface area of 3 cm^2 . The steel substrates were first sand blasted using $50 \text{ }\mu\text{m}$ particles, degreased in NaOH-saturated ethyl alcohol for 5 min., then etched in 25 wt. % HCl for 2 min. All solutions were made using distilled-deionized water and analytical grade chemicals.

Fe-Mo alloys were deposited from solutions containing 5 g/L or 9 g/L FeCl_3 , 40 g/L Na_2MoO_4 , 75 g/L NaHCO_3 and 45 g/L $\text{K}_4\text{P}_2\text{O}_7$ at 60°C . Ni-Mo alloys were deposited from solutions containing 9 g/L NiCl_2 , 40 g/L or 60 g/L Na_2MoO_4 , 75 g/L NaHCO_3 and 45 g/L or 65 g/L $\text{K}_4\text{P}_2\text{O}_7$ at 60°C . A Ti-Pt mesh was used as a counter electrode during electrodeposition.

The hydrogen evolution kinetics of the Fe-Mo electrodeposits were investigated in a standard electrochemical cell using an electrolyte commonly used for chlorate production, 300 g/L NaCl and 5 g/L $\text{K}_2\text{Cr}_2\text{O}_7$ at 80°C . The hydrogen evolution kinetics for the Ni-Mo alloys was examined in 1M NaOH at room temperature. A saturated calomel electrode (SCE) was used as a reference electrode while a flat Pt sheet served as a counter electrode.

All deposition experiments were performed using a function generator connected to a potentiostat/galvanostat. A computer was used to collect the current-voltage data for hydrogen evolution. These polarization curves were corrected for IR drop using standard techniques.

Scanning electron microscopy was used to characterize the as-deposited surfaces and to determine alloy composition using energy dispersive x-ray spectroscopy (EDS). Selected deposits were mounted in cross-section, polished and examined by optical microscopy.

3. Results and Discussion

3.1. Fe-Mo alloys

Although Ni-Mo alloys have much better polarization characteristics in 1M NaOH than Fe-Mo alloys, they cannot be used as cathodes in electrolytes commonly used for chlorate production since Ni is very catalytic towards the decomposition

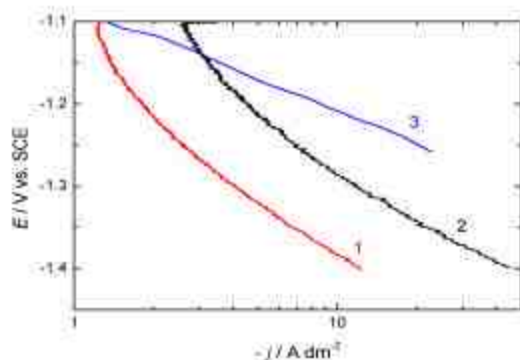


Fig. 1. Polarization characteristics of electrodeposited Fe-Mo alloys (2 and 3) and mild steel (1) in 300 g/L NaCl and 5 g/L $K_2Cr_2O_7$ at 80 °C: (2) 50 at.% Fe - 50 at.% Mo obtained by direct current and square wave pulse ($t_c = 10$ ms, $t_c/t_p = 1/3$); (3) 45 at.% Fe - 55 at.% Mo obtained by rectified alternating current.

of hypochlorite. This would decrease the current efficiency for hydrogen evolution and increase the oxygen content in the electrolyte (a maximum of 3 % oxygen is allowed in industrial plants). Fe-Mo alloys were electrodeposited by direct current, rectified alternating current, and square wave pulsed current to a thickness of about 20 μm . Their polarization characteristics in 300 g/L NaCl and 5 g/L $K_2Cr_2O_7$, the electrolyte normally used for chlorate production, are compared to that of mild steel in Figure 1.

It is clear from Figure 1 that electrodeposited Fe-Mo has a lower overvoltage for hydrogen evolution than mild steel. It is also clear that at current densities of commercial interest, the rectified AC waveform (3) produced a better performing alloy than either the DC or square wave pulse (2). An as-deposited view (a) and cross-section (b) of a typical Fe-Mo electrodeposit is shown in Figure 2. As is typical of alloys electrodeposited during significant hydrogen evolution, these films exhibit extensive cracking.

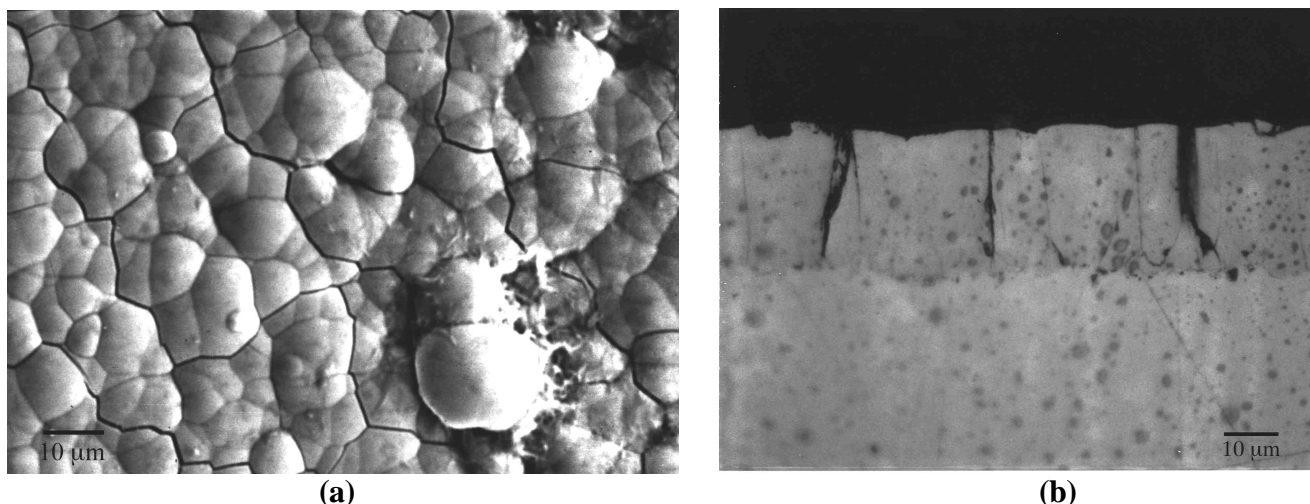


Fig. 2 As-deposited surface (a) and cross section (b) of Fe-Mo alloy deposited at 10 A dm^{-2} , DC.

It should be noted that the highest Mo content observed using DC or square wave pulse deposition was about 50 at. %, while Fe-Mo alloys containing up to 55 at. % Mo have been obtained by rectified AC. The current efficiency for alloy deposition was found to decrease with increasing effective current density for all deposition conditions. Typical efficiencies of about 45 % are obtained at 2.5 A dm^{-2} and decrease to about 12 % at 10 A dm^{-2} . Over this range of current densities, the Mo composition increased from 30 at. % to about 55 at. %.

A Fe-Mo alloy produced by rectified AC current to a thickness of about 20 μm (similar to deposit (3) in Figure 1) was exposed to long-term hydrogen evolution at a current density of 30 A dm^{-2} . Polarization diagrams recorded after 0 h (1), 24 h (2), 48 h (3) and 128 h (4) are shown in Figure 3. The hydrogen

overvoltage was found to decrease slightly with time of use. This is most likely the consequence of an increase in the total surface area due to hydrogen-driven ablation. Selected samples were tested under conditions of industrial chlorate production, using industrial test cells, at a current density of 30 A dm^{-2} . The test results for one of these samples are shown in Table 1. A cell voltage using mild steel cathodes in

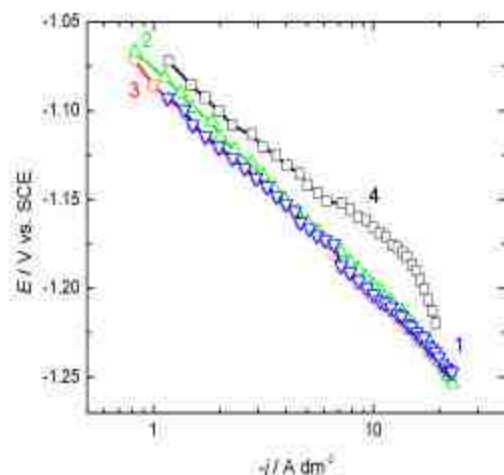


Fig.3. Polarization diagrams recorded on sample (3) of Fig. 1 after being on load in the electrolyte for chlorate production at $j = 30 \text{ A dm}^{-2}$ for (1) 0h, (2) 24 h, (3) 48h and (4) 128h

commercial cells is typically about 3.0 V. It can be seen in Table 1 that the average cell voltage using the Fe-Mo electrodeposit is about 2.65 V. Although test results showed significant improvement in cell voltage, the catalytic activity disappeared after about six months due to the co-deposition of iron during electrolysis. These electrolytes typically have a fairly high iron content as a consequence of mild steel corrosion during shut down for cell maintenance. The successful implementation of these cathodes into industrial plants would most likely be possible in newly built plants using iron-free electrolytes.

Table 1. Test results for one of the samples

DOL	NaCl (g/L)	NaClO ₃ (g/L)	Cell (V)	O ₂ %	-E _c / V vs. SCE
0	300				
1	201.9	212	2.59	2.00	1.38
2	106.6	461	2.65	1.80	1.43
10	122.6	489	2.65	2.10	1.44
23	120.6	481	2.66	3.08	1.43
33	113.4	501	2.66	2.76	1.44
47	111.6	445	2.63	3.24	1.42
60	109.5	427	2.63	2.76	1.42
82	140.9	492	2.65	3.58	1.43
101	122.2	502	2.65	3.20	4.16

101	300.0				
117	141.0	473	2.69	2.00	1.30
161	114.7	507	2.66	1.70	1.31
182	121.3	509	2.64	1.80	1.31
204	119.8	512	2.64	1.88	1.30
224	116.6	506	2.63	1.90	1.29
244	117.9	492	2.62	1.88	1.29

Initial cell gap: 1.4 mm

Initial Cathode Potential, E_c = - 1.322 V vs. SCE (DOL – Days on Load)

----- Restart: High O₂ due to bolt corrosion, cell gap=1.7 mm

3.2. Ni-Mo alloys

Ni-Mo alloys were electrodeposited using a pulsed square wave current (pulse/pause ratio was either 1/3 or 1/1) from a solution containing 40 g/L Na_2MoO_4 and 45 g/L $\text{K}_4\text{P}_2\text{O}_7$. Because of the very low current efficiency, the maximum deposit thickness was only about 2 μm . EDS analysis indicated that alloy composition increased from about 28 at. % Mo to 41 at. % Mo by increasing the effective current density from 2 Adm^{-2} to 10 Adm^{-2} . This is shown in Figure 4(a). The appearance of the coatings was similar to that shown for the Fe-Mo alloys in Figure 2. Polarization measurements for hydrogen evolution showed a decrease in overvoltage with increased molybdenum content. Figure 4(b) is a plot of the potential required to evolve hydrogen at a current density of 30 Adm^{-2} after 0.5 h (○) and after 3 h (●) of hydrogen evolution for alloys with varying Mo content. The catalytic activity for hydrogen evolution tends to increase (overvoltage decrease) with increased content of Mo. The data also suggests that the catalytic high-Mo coating (>40 at. %) may suffer from poor adhesion to the substrate and show limited stability during extended hydrogen evolution. The stability as a function of deposit thickness should be examined.

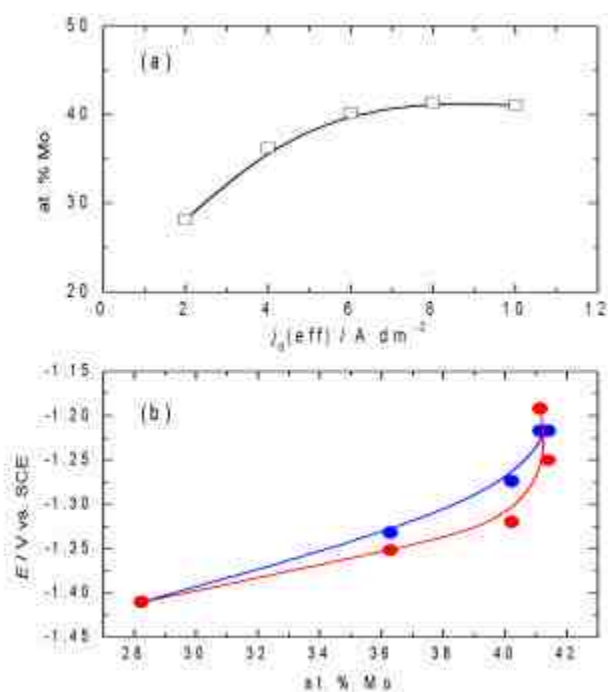


Fig. 4 (a) Dependence of Mo content in the alloy as a function of effective current density of deposition: (b) Dependence of potential for hydrogen evolution recorded at a current density of 30 A dm^{-2} after 0.5 h (○) and after 3 h (●) of hydrogen evolution as a function of Mo content in the alloy.

In order to improve the current efficiency for Ni-Mo alloy electrodeposition and increase the deposit thickness, the concentration of Na_2MoO_4 was increased to 60 g/L and $\text{K}_4\text{P}_2\text{O}_7$ was increased to 75 g/L. Using this electrolyte, the resultant Mo content of the alloy was about 40 at. % and was found to be independent of both current density and the applied current waveform. However, the current efficiency, increased from 1% to 6% as the current density was increased from 2 Adm^{-2} to 15 Adm^{-2} .

Hydrogen polarization curves for alloys electrodeposited at 6 Adm^{-2} (1), 10 Adm^{-2} (2) and 15 Adm^{-2} (3) are shown in Figure 5. The most favorable H_2 kinetics was obtained for the alloy deposited at 15 Adm^{-2} (3), although the composition of the other alloys was essentially identical. An attempt was made to correlate this behavior with an increase in the active surface area of the electrode by examining the cross-sections of these films.

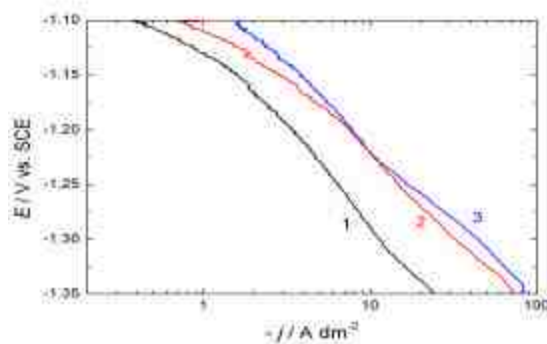


Fig. 5. Polarization curves for Ni-Mo alloys electrodeposited by DC regime at 6 A dm^{-2} (1), 10 A dm^{-2} (2) and 15 A dm^{-2} (3) for the same duration of deposition of 6 h.

The cross-sections of those electrodes used in the Figure 5 data are shown in Figure 6. It is clear that the thickness of deposit 1 is much less than that of deposits (2) and (3). It is also clear that the cracks in deposits (2) and (3) extend down to the steel substrate. The larger cracks in deposit (3) may lead to a larger electrochemically active surface area. Of course, this should be considered as a very rough approximation, since the number of cracks in all of these deposits is fairly large.

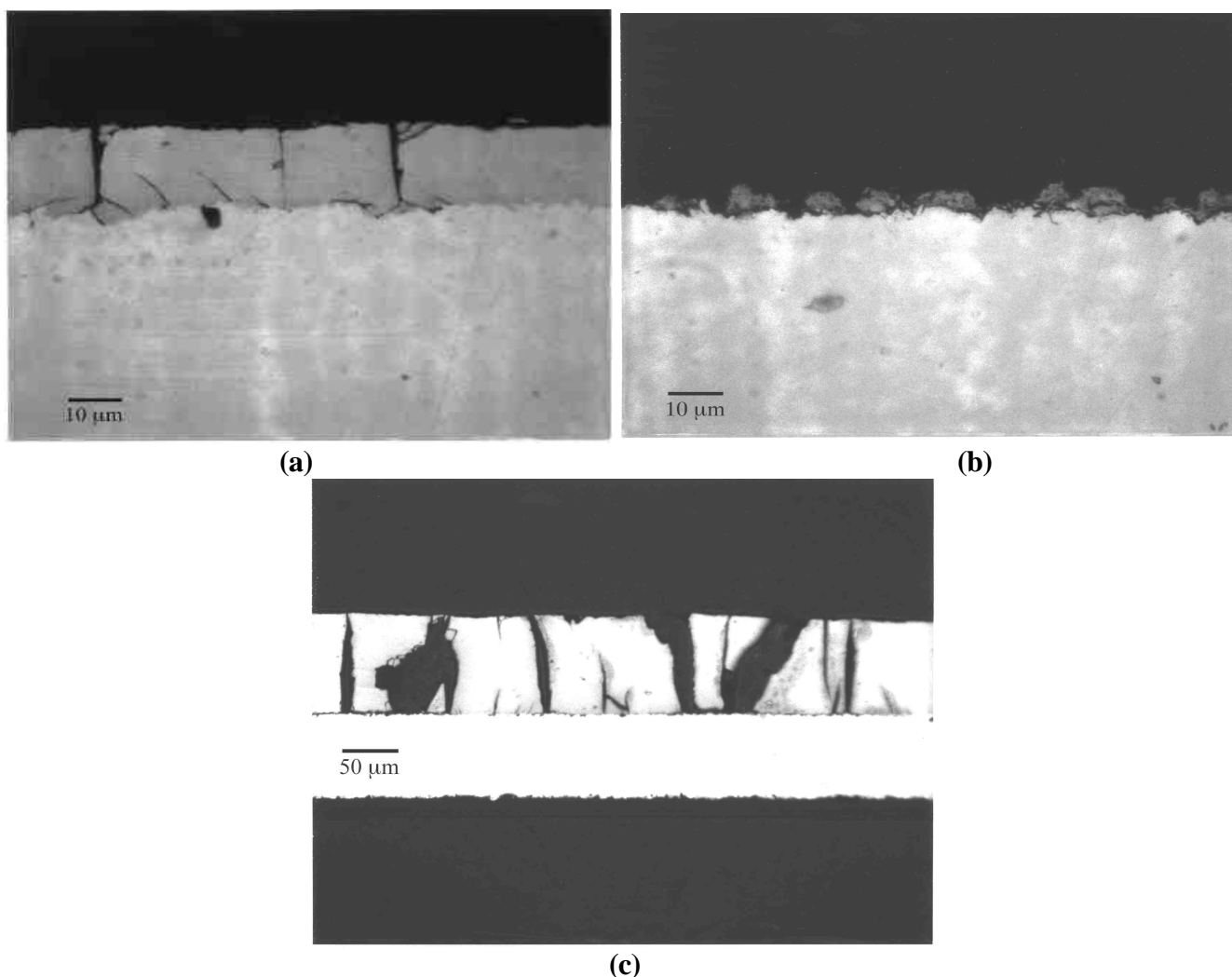


Fig. 6. (a) Cross section of coatings 1, (b) cross section of coatings 2 and (c) cross section of coating 3 from Fig. 5.

It is important to note that in comparison with a flat Pt surface, the Ni-Mo electrodeposits have a much lower overvoltage for hydrogen evolution (about 0.2 V lower than Pt) over an extremely wide range of current densities. It is presently not clear if this is due to higher catalytic activity for hydrogen evolution or simply the consequence of a higher electrochemically active surface area. In order to determine whether diffusion of hydrogen through open pores and cracks in the Ni-Mo coatings influences the kinetics of hydrogen evolution, preliminary electrochemical impedance spectroscopy (EIS) measurements were performed on an alloy deposited at a current density of 10 Adm^{-2} . The $Z'-Z''$ diagram recorded at -1.1 V vs. SCE (the current density for hydrogen evolution at this potential is about 0.5 Adm^{-2}) is shown in Figure 7. The fitting of experimental points (○) was performed by Armstrong's equivalent circuit⁷, with both, double layer (C_{dl}) and pseudo capacitance (C_p) being replaced by a constant phase element (CPE), as shown in Figure 8. The fitting curve is represented by the blue line in Figure 7 and the following parameters were obtained from this procedure: $R_\Omega = 2.83 \text{ } \Omega\text{cm}^2$; $R_F = 0.68 \text{ } \Omega\text{cm}^2$; $R_p = 5.93 \text{ } \Omega\text{cm}^2$; $C_{dl} = 0.099 \text{ Fcm}^{-2}$ ($a_1 = 0.62$) and $C_p = 0.0029 \text{ Fcm}^{-2}$ ($a_2 = 0.81$). a_1 and a_2 are exponents required for the two constant phase elements⁸, where $CPE_{dl} = Z_{dl}(j\omega)^{-a_1}$ and $CPE_p = Z_p(j\omega)^{-a_2}$. The extremely high values of both the double layer and pseudo capacitance, as well as low values of factors a_1 and a_2 indicate that hydrogen evolution takes place on a fairly high surface area electrode. One can conclude from this analysis that the diffusion of hydrogen through open pores and cracks in the coating does not limit the hydrogen evolution reaction on these electrodes. It should be noted that the same equivalent circuit has successfully been used for EIS analysis of cast Ni-Mo alloys⁹.

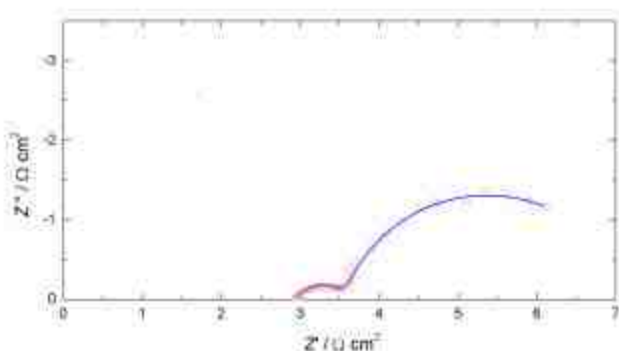


Fig. 7. $Z'-Z''$ diagram for hydrogen evolution on Ni-Mo alloy electrodeposited at a constant current density of 10 Adm^{-2} recorded at the potential of -1.1 V vs. SCE in 1 M NaOH in the frequency range from 0.001 Hz to 1000 Hz .

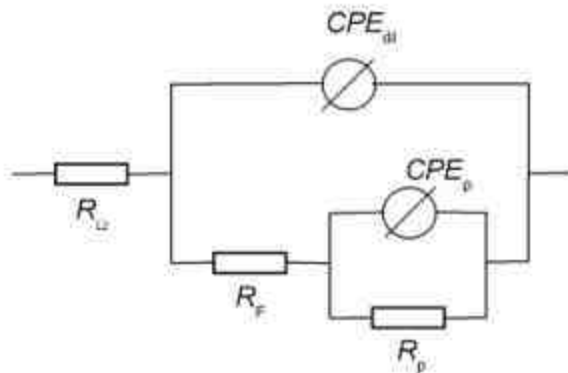


Fig 8. Randles equivalent circuit for hydrogen evolution with C_{dl} and C_p being replaced by Constant Phase Elements CPE_{dl} and CPE_p respectively.

The long-term electrochemical performance of a 20 μm thick Ni-Mo coating (electrodeposited at a DC current density of 10 Adm^{-2}) serving as a cathode for hydrogen evolution was examined. The hydrogen evolution kinetics and the cross-sections of the electrodeposits were periodically examined while the electrodes were undergoing hydrogen evolution at a current density of 10 Adm^{-2} at room temperature. The overvoltage for the hydrogen evolution reaction decreased slightly with time. The cross sections of this coating before

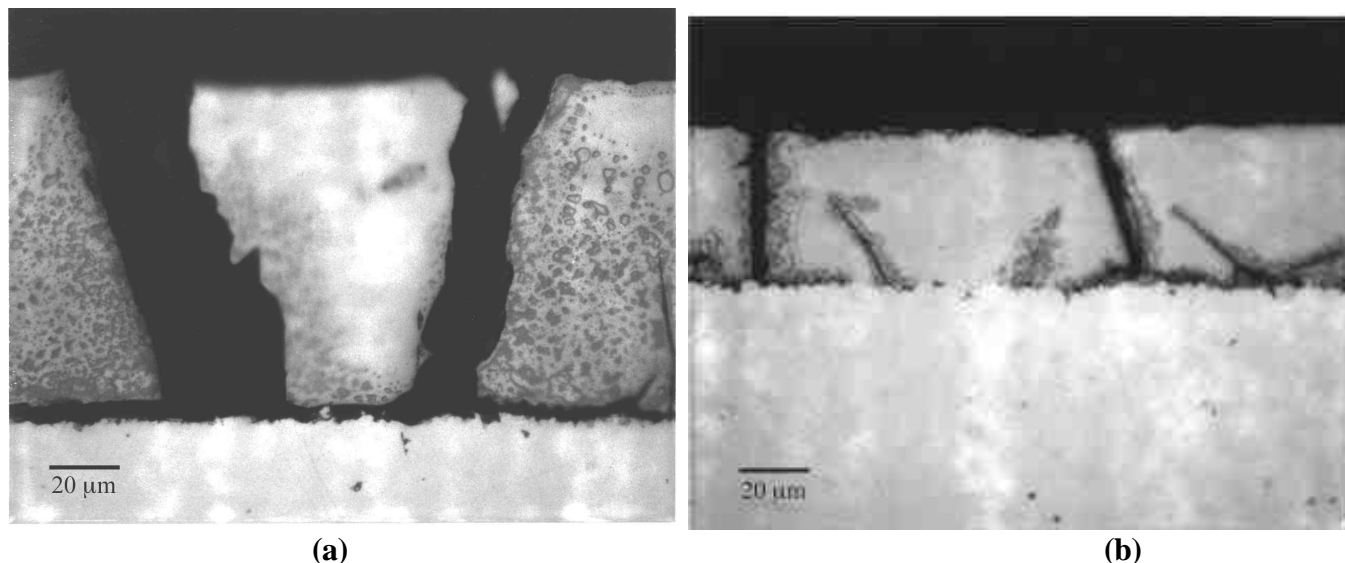


Fig. 9. Cross section of Ni-Mo coating electrodeposited at a current density of 10 Adm^{-2} DC immediately after deposition (a) and after 50 h of hydrogen evolution with $j = 10 \text{ Adm}^{-2}$.

exposure to hydrogen evolution (a) and after 50 h of hydrogen evolution (b) are shown in Figure 9. Prolonged hydrogen evolution increases the pore/crack size that allows electrolyte to seep in and hydrogen evolution to occur under the coating. This compromises the adhesion between the deposit and substrate and leads to failure of the coating during long-term operation.

It should be noted that similar behavior has not been observed for Fe-Mo coatings. This is most likely the consequence of better adhesion between Fe-Mo alloys and mild steel substrate. If Ni-Mo alloys are expected to be used in industrial applications of chlor-alkaline electrolysis, the cracks need to be eliminated or a substrate with better adhesion needs to be used.

4. Summary

Electrodeposited Fe-Mo alloys have a 0.15 V lower overvoltage for hydrogen evolution than mild steel cathodes when examined in an electrolyte commonly used for chlorate production. The long-term performance of such electrodes in an industrial test cell was satisfactory; however iron deposition, as a result of substrate corrosion products in the electrolyte, had a detrimental affect on catalytic activity.

Electrodeposited Ni-Mo alloys have high catalytic activity for hydrogen evolution in 1M NaOH solution. The overvoltage measured over a wide range of current densities was less than that measured on a flat Pt electrode. Under conditions of long-term hydrogen evolution, the combination of mild steel substrate and Ni-Mo coating was found to be unsatisfactory due to poor adhesion and subsequent coating failure.

References:

1. H.S.Myers, PhD Thesis, Columbia University (1961).
2. L.O.Case and A.Krohn, *J.Electrochem.Soc*, **105**, 512 (1958).
3. A.Krohn and T.Brown, *J.Electrochem.Soc*, **108**, 60 (1961).
4. J.R.Hall and J.T.Van Gemert, U.S.Patent 3,291,714 (1966).
5. N.Krstajic, K.Popov, M.Spasojevic and R.Atanasoski, *J.Appl.Electrochem*, **12**, 435 (1982).
6. M.Spasojevic, N.Krstajic, P.Despotov and R.Atanasoski, *J.Appl.Electrochem*, **14**, 265 (1983).
7. R.D.Armstrong and M.Henderson, *J.Electroanal. Chem*, **39**, 81 (1972).
8. J.R. Macdonald, *Impedance Spectroscopy Emphasizing Solid Materials and Systems*, John Wiley & Sons, New York, Chichester, Brisbane, Toronto, Singapore, 1987, p. 39.
9. J.M. Jaksic, M. V. Vojnovic and N. V. Krstajic, *Electrochim. Acta*, **45**, 4151 (2000).